Since January 2020 Elsevier has created a COVID-19 resource centre with free information in English and Mandarin on the novel coronavirus COVID-19. The COVID-19 resource centre is hosted on Elsevier Connect, the company's public news and information website.

Building and Environment 46 (2011) 2500–2511

Contents lists available at ScienceDirect

Building and Environment

journal homepage: www.elsevier.com/locate/buildenv

CFD simulation of airborne pathogen transport due to human activities

E.A. Hathway*, C.J. Noakes, P.A. Sleigh, L.A. Fletcher

Pathogen Control Engineering Institute, Department of Civil Engineering, University of Leeds, UK

ARTICLE INFO

Article history:
Received 6 April 2011
Received in revised form
27 May 2011
Accepted 2 June 2011

Keywords:
CFD
Bioaerosols
MRSA
Health-care associated infection

ABSTRACT

Computational Fluid Dynamics (CFD) is an increasingly popular tool for studying the impact of design interventions on the transport of infectious microorganisms. While much of the focus is on respiratory infections, there is substantial evidence that certain pathogens, such as those which colonise the skin, can be released into, and transported through the air through routine activities. In these situations the bacteria is released over a volume of space, with different intensities and locations varying in time rather than being released at a single point.

This paper considers the application of CFD modelling to the evaluation of risk from this type of bioaerosol generation. An experimental validation study provides a direct comparison between CFD simulations and bioaerosol distribution, showing that passive scalar and particle tracking approaches are both appropriate for small particle bioaerosols. The study introduces a zonal source, which aims to represent the time averaged release of bacteria from an activity within a zone around the entire location the release takes place. This approach is shown to perform well when validated numerically though comparison with the time averaged dispersion patterns from a transient source. However, the ability of a point source to represent such dispersion is dependent on airflow regime. The applicability of the model is demonstrated using a simulation of an isolation room representing the release of bacteria from bedmaking.

1. Introduction

Transmission of infection by airborne routes is widely recognised as a key factor in the spread of many diseases including Tuberculosis, Severe Acute Respiratory Syndrome (SARS) and Influenza, and control strategies involving ventilation design and face masks for patients and staff are widely advocated [1]. However, despite a growing body of evidence that aerial transmission may be important, there is little research on strategies to control airborne transport and environmental contamination arising from pathogens that colonise the skin, such as Methicillin Resistant *Staphylococcus aureus* (MRSA). Although MRSA is primarily transferred via contact spread it may also colonise the nasal passages as a result of airborne contamination [2], spreading to the skin and potentially resulting in further transfer to wounds or ingestion [3]. Since MRSA has the ability to survive for several months on hospital surfaces [4,5] any airborne particles depositing on surfaces have the potential to create long term reservoirs of infectious material that can be transferred by touch to new patients. Boswell and Fox [6] showed surface contamination reduced when portable air cleaning devices were deployed, clearly indicating that airborne transport plays a role in the dispersion of MRSA in the environment. The release of particles contaminated with MRSA into the air may occur from the skin which is shed during routine activities such as walking [7,8], bedmaking [9–11] and undressing and washing [7,12,13]. In such cases dispersion does not occur from a single point in space, as a respiratory release. Instead the dispersal of bacteria will vary in spatial location and intensity depending on the activity. Understanding this release, and the likely environmental contamination that results, is key to developing appropriate interventions for reducing the aerial transmission of such pathogens.

In this paper we consider the development, validation and application of appropriate Computational Fluid Dynamics (CFD) models for evaluating the airborne dispersion of pathogens in hospital environments due to activity. The study has three main objectives to assess the transport model assumptions, source definition and applicability of CFD models in a typical ward environment:

1. *Experimental validation of modelling techniques for bioaerosol transport*: bioaerosol experiments are conducted in a climatically controlled chamber in order to validate the transport

* Corresponding author. Present address: Department of Civil and Structural Engineering, University of Sheffield, Mappin Street, Sheffield S1 3JD, UK. Tel.: +44 0 114 2225702; fax: +44 0 114 2225700.
E-mail address: a.hathway@sheffield.ac.uk (E.A. Hathway).

0360-1323/$ – see front matter © 2011 Elsevier Ltd. All rights reserved.
doi:10.1016/j.buildenv.2011.06.001

simulations within the CFD model using both passive scalar and Lagrangian particle tracking for comparison. Two different bioaerosol sources are used, a single point source and a linear source which releases bioaerosols across its length.

2. *Numerical validation of a zonal source concept*: The concept of the zonal source is to represent the complex releases of bioaerosols that vary through time and space in a real hospital environment with an appropriate zone that encompasses the spatial volume of the release. The source is then effectively a time averaged representation of a random source that moves within the zone. The methodology is numerically validated by comparing the dispersion patterns from a steady state release of bioaerosols over a zonal source with the dispersion from a source that traverses the space with time.
3. *Sensitivity analysis in a realistic application*: The geometry of the zonal source is designed to encompass the region the bioaerosol release takes place. For certain activities the exact dimensions of the zonal source will be difficult to define. Therefore the sensitivity of the zonal source to the definition of size and shape was studied based on the simulation of an isolation room. This was also compared to the sensitivity of the point source release to the injection location to draw conclusions about the appropriateness of both source representations in modelling pathogen dispersion

1.1. CFD modelling of pathogen dispersion

CFD modelling is an increasingly popular approach that has the potential to give some insight into the airborne dispersion of infectious microorganisms and the effectiveness of control strategies. Many studies focus on ventilation design and range from single and multibed ward spaces [14–17] to high risk areas such as operating theatres [18], treatment rooms and isolation rooms [19,20]. Other related applications include outdoor pathogen dispersion in the SARS outbreak [21] and assessing air disinfection device performance [22]. However the validity of such simulations relies on appropriate definition of a pathogen source and an appropriate model for the transport of the pathogen through the air.

Pathogen transport is typically approached in one of two ways. A passive scalar model treats airborne pathogens as a concentration that is transported with the air. Particle properties are approximated through a diffusion coefficient, but the actual particle dynamics are not incorporated. As such the model tends to be used for demonstrating ventilation efficacy [23] and in the context of pathogens is regarded as acceptable for simulating respiratory diseases where the particle size is below 2 mm [14,15]. The airborne pathogen concentration can easily be presented and is ideal for showing steady state behaviour where there is a continuous source. Alternatively the movement of individual particles can be tracked using a Lagrangian particle tracking model. This considers the forces on particles due to their mass and momentum, producing path lines that are dependent on particle size and density as well as the local airflow. In theory the technique can be applied to any particle size and can also be used to evaluate deposition patterns. The main limitation of the approach is that tracking is time dependant and it is therefore difficult to determine steady state airborne contaminant distributions.

Previously passive scalar validation has focused on experiments using tracer gases, with good comparison seen for overall ventilation efficiencies for various designs [23] as well as the tracer distribution in a space [24,25] except very close to the source [26]. Particle tracking models have been compared against experiments conducted over a wide range of particle sizes. Particle mass concentration is well represented provided a large enough number of particles are injected in the model [27,28], while good correlation with particle distribution has been demonstrated up to 10 mm [29,30] except in areas of high gradients such as close to the source or at air inlets. Recent studies have indicated that including the effects of turbulent diffusion through a Discrete Random Walk (DRW) model improves the predictions, with Wan et al [31] showing good vertical and horizontal distribution of particles using a DRW approach, although Lai and Chen [32] indicate that the model is highly sensitive to grid size particularly when modelling particle deposition.

While these studies demonstrate the ability of both approaches to represent general contaminant behaviour, they are not compared directly to bioaerosol dispersion, most probably due to the difficulty in conducting such experiments. A number of studies provide indirect evidence by showing that bioaerosols compare well to experimental particle tracers [33,34]. Some authors have also attempted to validate by comparison with microorganism deposition in real environments such as operating theatres [35] but found that the lack of control in the experiment and inability to incorporate the movement of people into the CFD model resulted in discrepancies between the two. Apart from some limited data in Noakes et al. [33], there is a notable absence in the literature of clear comparisions between airborne microorganism behaviour and CFD models conducted under controlled conditions.

The source definition is also an important consideration in a CFD model. As much of the current literature focuses on respiratory infections, models tend to define the contaminant injection as a point source located at the patient's head. While this approach is appropriate in many cases it is clearly not valid where pathogens are released over a significant spatial zone, such as the dispersion of MRSA through activity. Some studies of operating theatres have recognised this [18,36] and represented dispersal from the skin by a plane rather than a point source, but offered no validation of the method.

2. Methodology

2.1. Experimental chamber and methods

Experiments were carried out in a 32.25 m^3 (3.35 × 4.26 × 2.26 m) mechanically ventilated chamber, which is similar in size to a single bed hospital room. The chamber is operated at a negative pressure of approximately −25 Pa and air is HEPA filtered on the supply and extract. Air was supplied through a low level wall mounted diffuser (Inlet A, Fig. 1) and extracted through a high level diffuser on the opposite wall (Outlet A). The room was empty except for the bioaerosol source and sample tubes, there were no heat sources in the space and the room air was maintained at 21(±1.1) °C and 50(±20)%RH.

Bioaerosols were generated using a six jet collison nebulizer (CN 25, BGI Inc, USA) operated at 12 l/min with a maintained pressure of 20 psi. These were injected into the space via a 34 mm diameter plastic pipe that terminated with 3 parallel sets of 4 holes, spaced equally apart around the pipe and located in the centre of the room to simulate a *point source*. A *linear source* was also created using 8 repeats of the point source spread equally over a distance of 750 mm. A pure culture of *Serratia marcescens* (ATC274) was used to create the bioaerosols. This is a non fastidious organism that grows on general purpose media and performs comparably with other vegetative organisms when sampled from the air during controlled tests [38]. The nebulised liquid was created out of a 2 ml aliquot with concentration of approximately 1×10^9 per ml suspended in 100 ml of sterile distilled water.

For passive scalar validation the chamber was ventilated at a constant rate of either 6 or 12 ac/h for 4 h during which time the nebulizer was operated continuously. Forty five minutes were

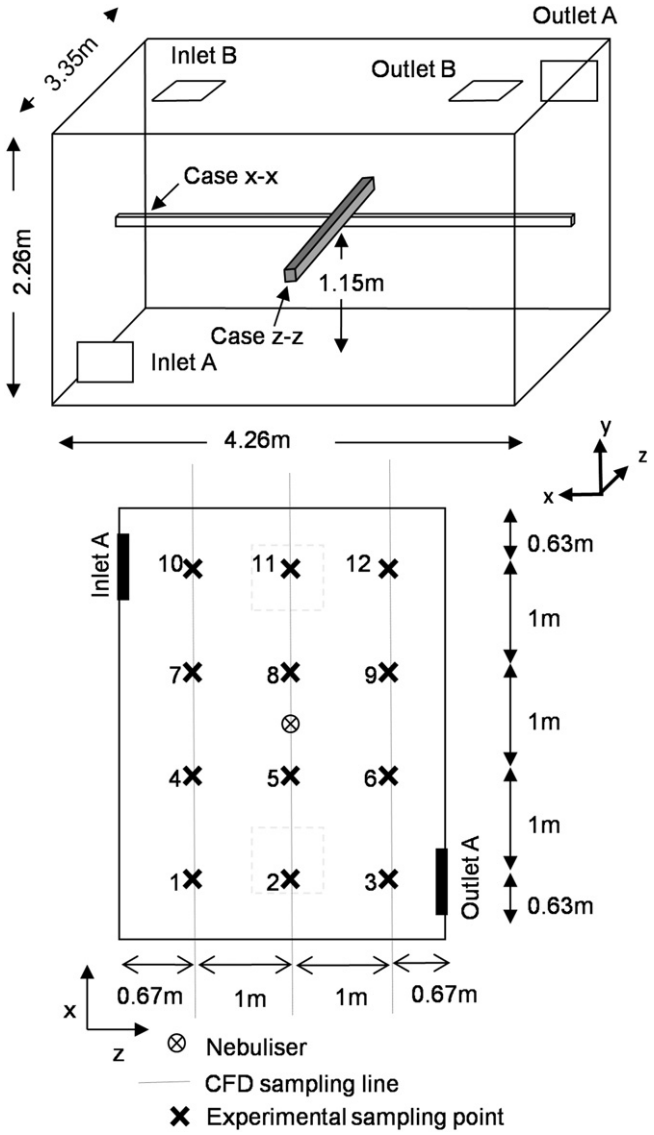

Fig. 1. Schematic of the controlled experimental chamber (top). Plan of the experimental chamber showing sample points and equivalent CFD sample lines for comparison (bottom).

allowed for the ventilation air and bioaerosol concentration to stabilise, then air samples were taken sequentially from each of the 12 sampling locations (Fig. 1) every 10 min. Air was sampled through 5 mm plastic tubes using an Andersen sampler (Anderson Instruments, USA) and impacted onto 90 mm diameter plastic agar plates filled with Nutrient Agar. These were incubated for 24 h at 37 °C and the resulting colony forming units (cfus) were counted and subjected to positive hole correction [39] before quantifying the concentration of *Serratia marcesens* in cfu/m^3. Twelve sample repeats were carried out at each 12 locations spread over three distinct experiments.

Deposition of bioaerosol particles on the chamber floor was measured for comparison with the Langrangian particle tracking model. In these experiments 21 nutrient agar plates were spaced out across the floor. The room was ventilated at a constant rate of 3 ac/h for 3 h with bacteria injected as above for the first 1.5 h. Air samples were taken every 20 min (equivalent to 1 air change rate). The air samples followed the same procedure as above but used only one sampling point close to outlet A. Following the experiment all the plates were incubated for 24 h at 37 °C and the colonies counted.

2.2. Numerical airflow simulation

CFD simulations were carried out using Fluent 6.2 (ANSYS). All models were based on the basic geometry of the experimental test chamber with some variation (Fig. 1). The computational grid varied slightly due to these variations. However, for all models it was in the region of approximately 600,000 tetrahedral cells with refinement around the boundaries and bacterial source. Grid dependency and mesh quality was ensured. A standard k-ε turbulence model was used with enhanced wall treatment and a no slip condition applied at the wall. Two different air flow regimes (A and B) were applied as shown in Fig. 1. In ventilation regime A the low-wall supply air inlet was defined as a series of velocity profiles to represent the angled louvers and the high-wall extract as a zero pressure boundary. In ventilation regime B the ceiling mounted four-way diffuser was represented as a box that projected 60 mm into the space with a velocity boundary condition on each side on the box angled at 45°. The ceiling mounted extract was again defined as a zero pressure boundary in models 1 and 2, and with a negative pressure in model 3. Three models were developed to achieve the study objectives as follows:

Model 1: The simulation was designed to replicate the conditions in the experimental studies. The model was treated as isothermal as there were no heat sources and the incoming air temperature and humidity was controlled. The ventilation was regime A only, and simulations were carried out at three air exchange rates; 3, 6 and 12 ac/h.

Model 2: The second model was used to carry out the numerical validation of the zonal source concept. The geometry was as model 1, and the simulations were again isothermal. In this case ventilation regimes A and B were both considered with all simulations at an air change rate of 6 ac/h.

Model 3: The final study applied the concept to a realistic room scenario. The model was refined to include a table, bed including reposed patient and sink in order to represent an isolation room (Fig. 2). Heat sources were applied to the lights (50 W/m^2) and the patients (60 W/m^2). The air change rate was 10 ac/h with an extract of −10 pa in line with UK design guidance for isolation rooms [40].

For all models second order discretisation of the governing equations was used and solutions found using a segregated implicit solver. Convergence was defined when residuals were less than 5×10^{-4} and the net imbalance of mass flow was less than 0.1%. The airflow is solved in steady state, although for the numerical validation there is a need to solve the time dependent release and transport of bioaerosols this is based on a steady state solution to the air flow.

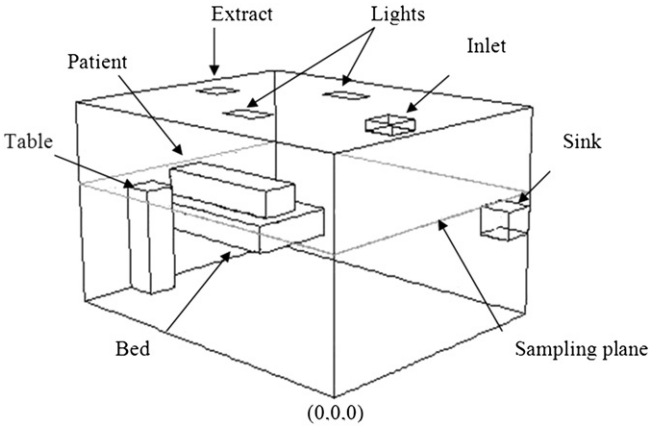

Fig. 2. Isolation room geometry (model 3).

2.3. Bioaerosol transport

As bioaerosols in the hospital environment can range from being droplet nuclei less than 1 μm in diameter to flakes of skin squame between 4 and 22 μm [12,41] a range of particle sizes was required in the modelling studies. Model 1 validates bioaerosol transport against experimental studies using a nebulizer designed to produce aerosols with a mass median diameter of 2.5 μm and a geometric standard deviation of 1.8 [42]. In model 2, for the numerical validation and application, the simulations considered particles sized 5 μm and 10 μm to represent skin squame.

2.3.1. Passive scalar model

Since the injected mass median diameter in the experiments is 2.5 μm and aerosols are likely to evaporate further it is reasonable to assume the particles will follow the behaviour of a passive scalar and can therefore be represented using the scalar transport equation:

$$\frac{\partial \phi}{\partial t} + div(\phi \mathbf{u}) - div(\Gamma grad\phi) = 0 \quad (1)$$

Here ϕ is the concentration of microorganisms per unit volume (quantity.m^{-3}); $\mathbf{u}$ is the velocity vector (u,v,w) of the air (m s^{-1}); and Γ is the diffusivity (kg m^{-1} s^{-1}). Natural decay of viable microorganisms in the space is not considered in this case. The diffusivity of the bioaerosols is set to 1×10^{-7} kg m^{-1} s^{-1} to represent the low diffusion of particles.

2.3.2. Langrangian particle tracking model

In order to study the transport and deposition of larger particles a Lagrangian model is adopted where the trajectory of a particle is found by considering the change in particle velocity (u_p) due to the particles inertia, gravity, and drag forces

$$\frac{\partial u_p}{\partial t} = F_D(u - u_p) + \frac{g_x\left(\rho_p - \rho\right)}{\rho_p} + F_x \quad (2)$$

The first term on the right hand side $F_D(u - u_p)$ is the drag force per unit particle mass. u is the velocity and F_D is defined using the spherical drag law (equation (3)). The second term represents the gravitational force where g is the gravitational acceleration and ρ is the density. F_x is used to incorporate additional forces and equals zero in this study. The subscript term p refers to the particle and unsubscripted terms refer to the air.

$$F_D = \frac{18\mu}{\rho_p d_p^2}\frac{C_D \mathrm{Re}}{24} \quad (3)$$

Where is theμ molecular viscosity of the fluid, d_p is the diameter of the particle, Re the Reynolds number and C_D the drag coefficient for spherical particles. A Discrete Random Walk (DRW) model is used to account for the effect of turbulent dispersion on the particle trajectories. This includes the fluctuating component of the velocity due to turbulence u' to provide the instantaneous fluid velocity u as shown in equation (4). The fluctuating component is assumed to be isotropic and to follow a Gaussian distribution. It can therefore be expressed based on the turbulent kinetic energy, k, and a random number, ζ as given in equation (5).

$$u = u + u' \quad (4)$$

$$u' = \zeta\sqrt{\overline{u'^2}} = \zeta\sqrt{\overline{v'^2}} = \zeta\sqrt{\overline{w'^2}} = \zeta\sqrt{2k/3} \quad (5)$$

2.4. Injection definition

For each of the three objectives outlined above it was necessary to consider different types of injection. These are summarised in Table 1 for scalar sources. For numerical validation two cases are considered. Case x–x spans the room in the x direction, and z-z in the z direction as detailed in the table. The transient source in these cases is defined as a small cube that moves through the space, and the zonal source encompasses the entire volume the transient source moves through.

Passive scalar models all assumed a constant release of 500 cfu/s with a momentum source of 0.1 N m^{-3}, over the source zone throughout the simulation. Transient simulations were run for the entire time it took the source to traverse the space, 3600 and 2600 s for the x–x and z-z source respectively. The bioaerosol concentrations in the room were exported every 100 s to calculate the time averaged results at each cell for comparison to the steady state models.

The particle tracking used the same source definitions as given in Table 1 except sources are points, or lines, passing through the centre of the volumes for model 1 and 2. All sources released at least 6700 spherical particles for each size range, as a sensitivity study indicated this was adequate. An uncoupled solution for particle tracking was used. For the transient source 100 particles were injected per time step (1s during injection) and the total number injected then used for the equivalent zonal and point source. Tracking was run for a further 18,000 s to ensure the majority of particles were removed from the air either by extraction

Table 1
Definition of airflow and geometry of bioaerosol sources for all models. In all cases a small momentum source is applied to expel the bioaerosols into the air.

Objective	Airflow		Injection		
	Regime	AC/h	Name	Size	Location
1. Experimental validation of modelling techniques for bioaerosol transport	A	3, 6, and 12	Point Source	0.1 m^3	Central on plan, at height of 1.15 m
			Linear Source	0.1 × 0.1 × 1.2 m	Spanning from centre to $x = 0.45$ m
2. Numerical validation of the concept of the zonal source	A and B	6	Point Source	0.1 m^3	Central on plan, at height of 1.15 m
			Zonal Source	0.1 × 0.1 × 3.0 m	Spanning from: $z = 0.42$ to 3.42
			Case z–z	0.1 × 0.1 × 3.6 m	and $x = 0.33$ to 3.93
			Case x–x		
			Transient Source	0.1 m^3	Travelling at 1.2 x10^{-3} m/s:
			Case z–z		-from $z = 0.42$ to 3.42
			Case x–x		-from $x = 0.33$ to 3.93
3. Sensitivity analysis and application	B	10	Point Source × 9 Zonal Source	0.1 m^3	See Fig. 3
			Case Zu (x3)	1.8 × 0.5 × 0.1, 0.4 or 0.7	Above patient,
			Case Zl (x3)	2.0 × 1.1 × 0.4, 0.7 or1.0	Above bed and encompassing patient

or deposition. With the zonal and point source the solutions were run for 1.5×10^5 steps after injection to ensure less than 10% particles remained suspended in the air.

For the experimental validation the particle sizes used were based on the manufacturers' literature [42] for the Collison nebulizer as discussed in 2.3, with sizes between 0.78 and 9 μm, injected with a mass flow rate of 10^{-9} kg/s and a density of 1000 kg/s. For the later numerical validation and application particles of 5 and 20 μm in diameter were defined.

The sensitivity analysis conducted with model 3 was based on 15 different sources. Nine point sources were located over the top of the bed at a height of 1.4 m along the centre line, and 1.2 m along the edge of the bed (Fig. 3). Six zonal sources of varying size were defined around the bed the dimensions of which are described in Table 1. Three sources labelled Zu cover only the top of the patient, and three sources labelled Zl cover the bed and the patient. The three variations are changes in height of the source. For particle tracking 3 simulations were carried out for each source definition with particle diameters of either 5, 14, or 20 μm.

3. Results

3.1. Experimental validation of CFD methodology

Figs. 4–6 show the comparisons between the experimental measurements of bioaerosol concentration and the CFD results. These show the concentrations exported from the simulations along three lines alongside the equivalent experimental samples at a height of 1.15 m (see Fig. 1). Results are normalized in order to compare the pattern of dispersal between the simulations and

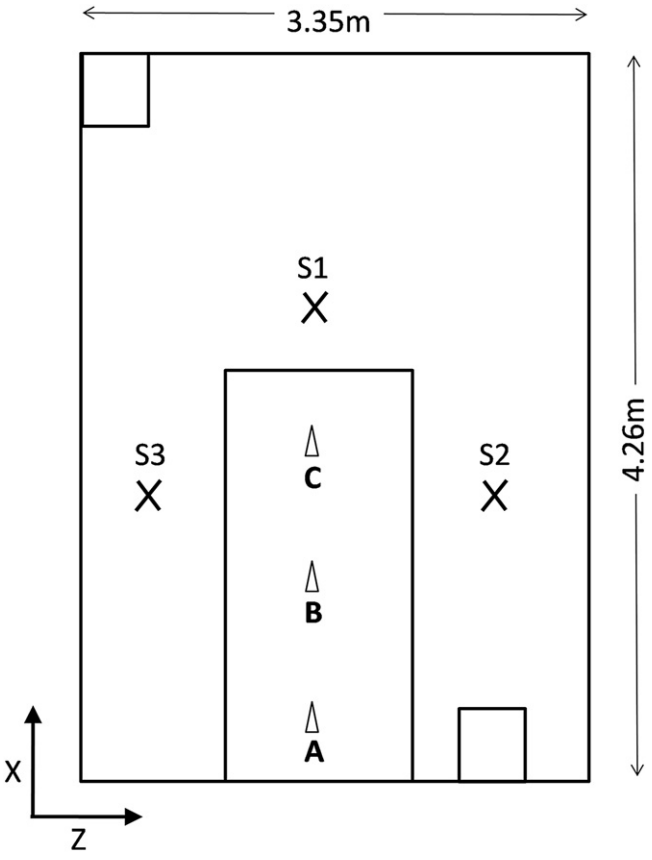

Fig. 3. Plan view of model 3 (isolation room), showing point source (A–I) and sampling locations (S1, S2, S3).

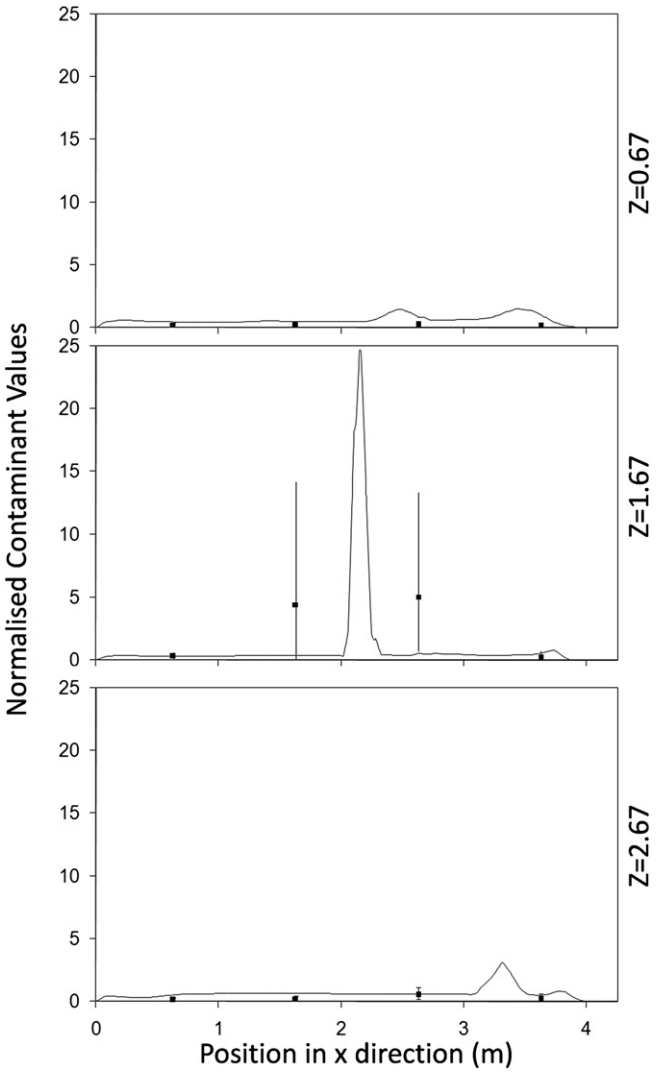

Fig. 4. Normalised concentrations from the CFD simulations (lines) compared to experimental samples (points with error bars) along 3 separate lines passing through the test chamber for test run at 6 ac/h using a central point source.

experiments. For the experimental data a normalised value was found for each experiment and the average of all three experiments used for comparison. For the simulations the values are normalised using the average from all three lines. As can be seen in Figs. 4–6 there is a large variation in bioaerosol measurements which is likely to be due to loss of viability during nebulisation and sampling. However, despite this variation there is clear tendency for the simulation to follow the same dispersion pattern as found experimentally. In both simulations and experiments there is a tendency for the contaminant to be entrained into the inlet air stream at higher air change rates (Fig. 7). This pull towards the inlet was also confirmed using smoke tests. It was not possible to take experimental samples directly at the source, although based on interpolation it appears that there is a tendency to overestimate the concentration at this location in the simulations which has previously been noted by Zhang et al. [26].

The experimental deposition of microorganisms on the floor was calculated as a percentage of the total airborne count. This was quantified by extrapolating from the summation of all air samples. The airborne count was not calculated from the nebulizer concentration as the nebulising process can cause a significant loss of viability [41]. The deposited fraction was then found by

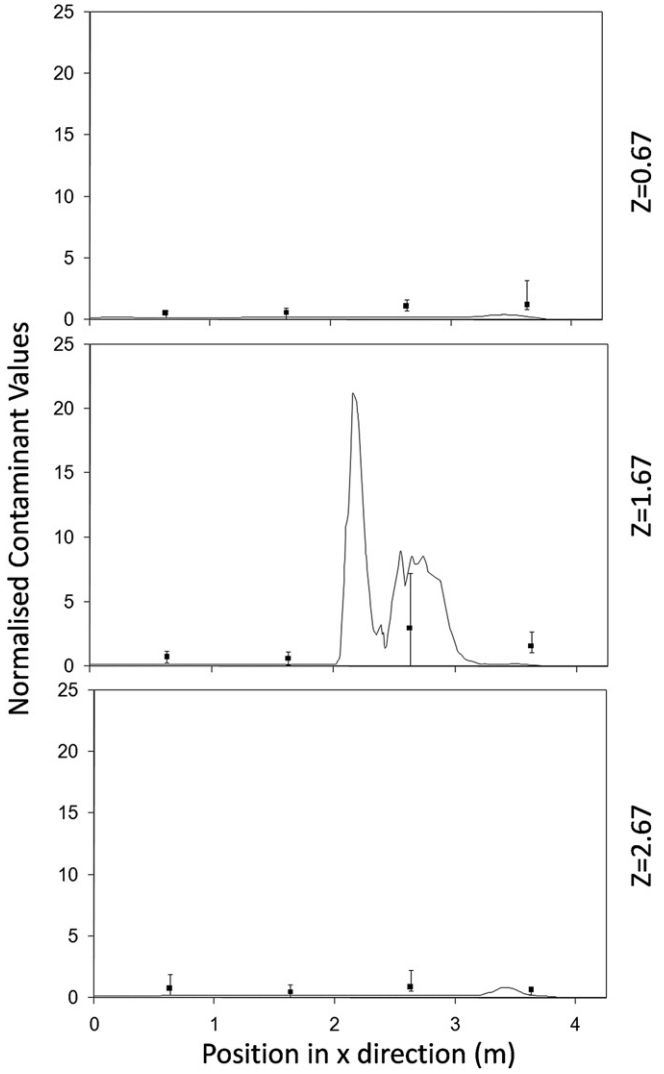

Fig. 5. Normalised concentrations from the CFD simulations (lines) compared to experimental samples (points with error bars) along 3 separate lines passing through the test chamber for test run at 12 ac/h using a central point source.

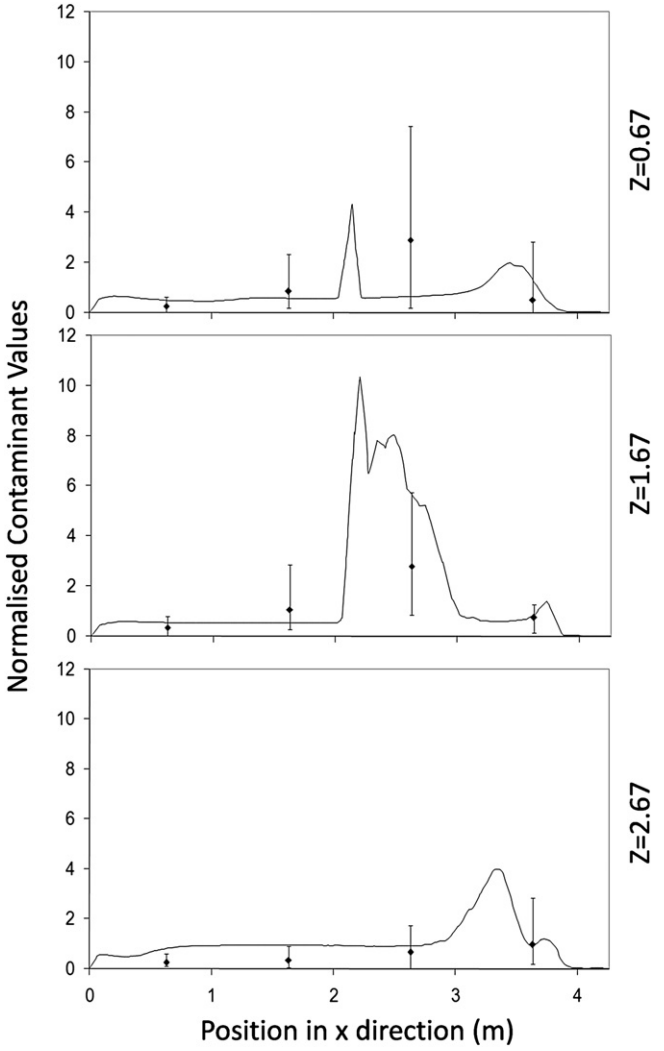

Fig. 6. Normalised concentrations from the CFD simulations (lines) compared to experimental samples (points with error bars) along 3 separate lines passing through the test chamber for test run at 6 ac/h using a linear source.

averaging the number of colonies formed on each of the 24 plates, and multiplying up to assume the same deposition over the whole floor. In the CFD simulations the total number of particles depositing on the floor was found as a fraction of the injected quantity. Deposition values were found by a exporting data for the time and co-ordinates of particles "trapped" on the floor zone. Comparison between experimental and CFD depositions are shown in Table 2. Once the DRW model was incorporated the

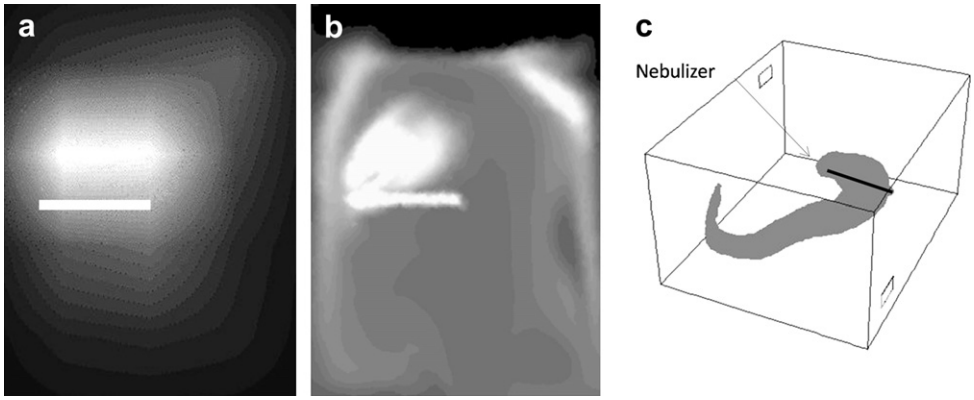

Fig. 7. Contours of bioaerosols from the linear source. Values on plane $y = 1.15$ m a) experimental results, b) CFD results. c) Plume showing 3D dispersal pattern from CFD results. Orientation as plan in Fig. 1.

Table 2
Deposited particle fractions found experimentally and using Lagrangian Particle Tracking based on eitherbulk flow or incorporating the DRW model.

	Experimental	Bulk Flow	DRW
Percentage deposited	9.1	0.4	14.2

values of deposition were of the same order of magnitude as the experimental values.

3.2. Numerical validation of the zonal source

As discussed in Section 1 the zonal source seeks to represent the transient release of bacteria over the time and space in which the activity occurs, creating a zone with a consistent average bioaerosol release spread across it. The purpose of this source is to represent the average behaviour of a complex release from a source that moves through the space and hence is a replacement for a time dependant simulation of a transient source that moves through the zone. The numerical validation therefore compares the dispersion of bioaerosol from a zonal source in a steady state model with that from an injection of bacteria which moves through a zone. A point source simulation is also used for comparison.

The transient source is compared to both the point and zonal source for the two airflow regimes at 6 ac/h across two planes in Figs. 8–11 with relevant correlation coefficients given in Table 3. Spearmanns Rho correlation was used as the data did not follow a Gaussian distribution. The results from the transient source were averaged over 2600 s based on results exported every 100 s. Correlations were then carried out using the values in comparable cells, based on over 10,000 cells. It is clear from the figure that the zonal source more accurately represents the transient source than

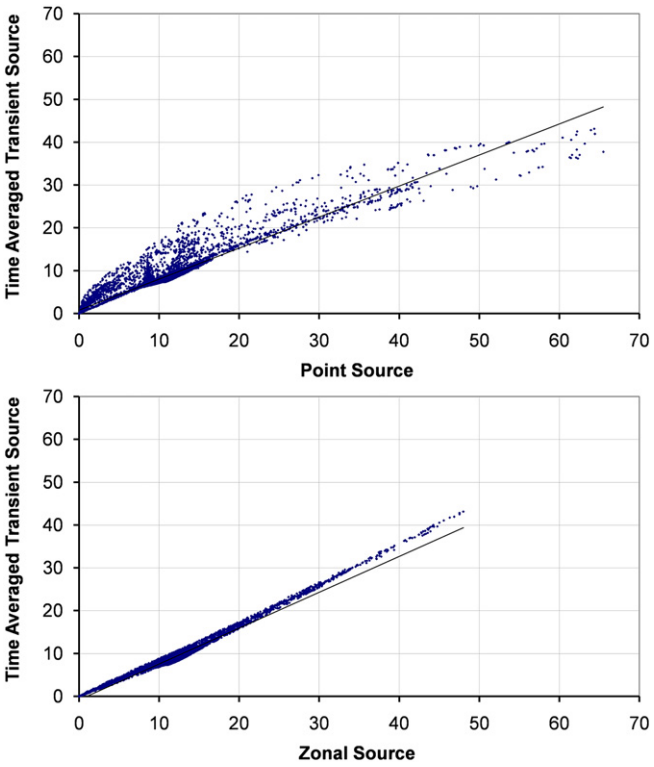

Fig. 9. Scatterplots showing comparisons between the time averaged dispersion from a transient source and a zonal or point source on the plane $y = 1.60$ m with source case x–x.

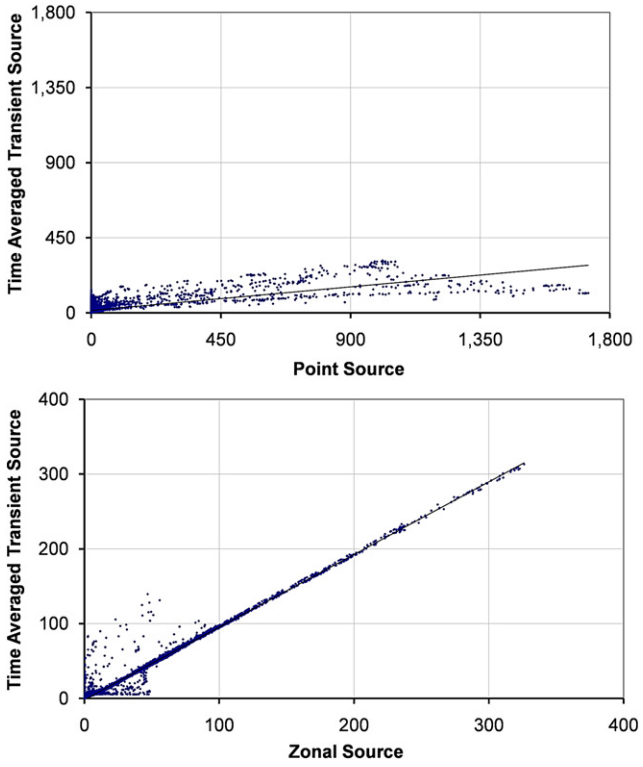

Fig. 8. Scatterplots showing comparisons between the time averaged dispersion from a transient source and a zonal or point source on the plane $y = 1.15$ m with source case x–x.

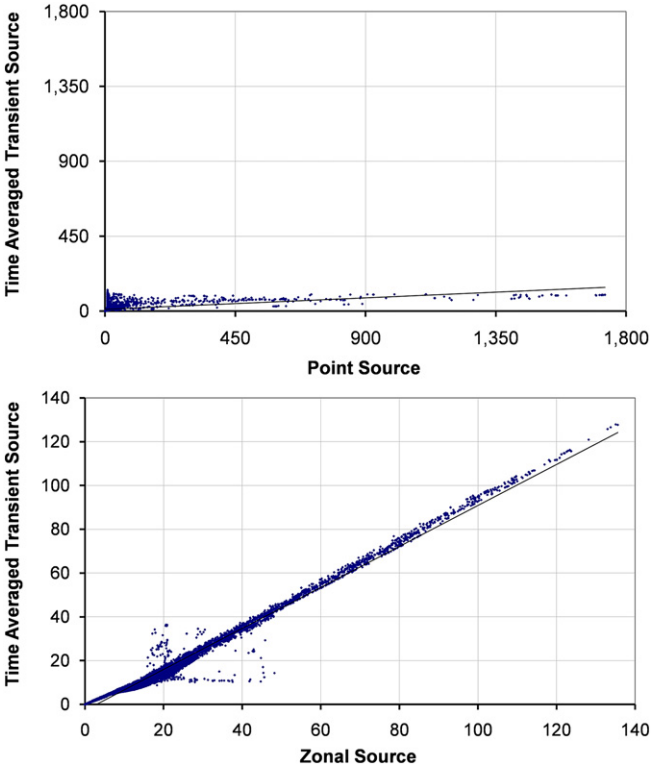

Fig. 10. Scatterplots showing comparisons between the time averaged dispersion from a transient source and a zonal or point source on the plane $y = 1.15$ m with source case z–z.

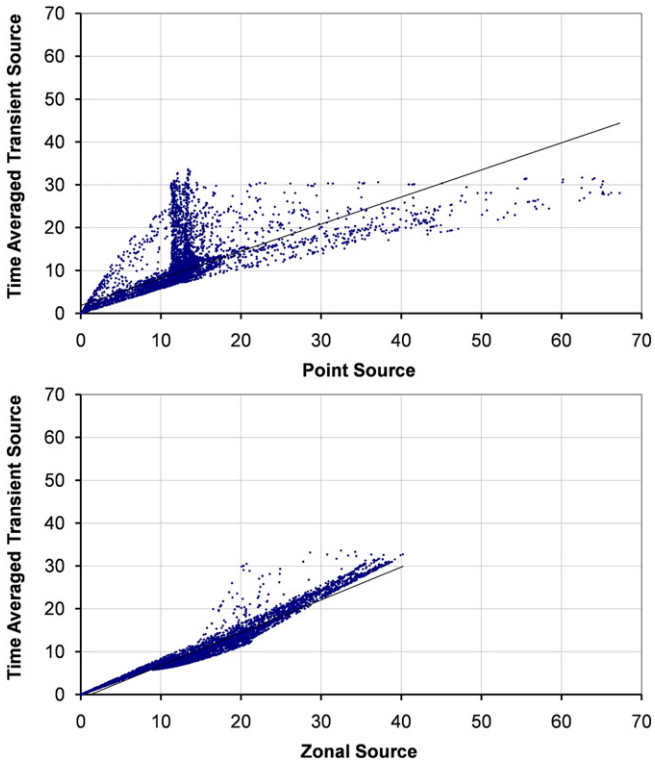

Fig. 11. Scatterplots showing comparisons between the time averaged dispersion from a transient source and a zonal or point source on the plane $y = 1.60$ m with source case z–z.

a single point source. The point source heavily over estimates the concentrations in certain locations. More importantly on the sample plane at 1.60 m the spread of values is much greater using the point source, whereas the zonal source much more accurately follows the time averaged results from the transient source (Figs. 9 and 11).

Using the Lagrangian particle tracking model the total deposited fraction was calculated and compared as well as comparing the pattern of deposition across the floor. The pattern of deposition was based on the concentration of particles depositing in 0.2 m^2 zones. The total deposition is comparable between all sources as shown in Table 4, however the deposition from the transient source in Regime B is higher. Fig. 12 compares the pattern of deposition from the simulations across the room for particles sized 5 and 10 μm. It is clear the transient source results in a greater deposition towards the inlet but overall there is similarity to the zonal source.

Table 3
Comparison of concentration contours between Transient source and Zonal or Point source models using Spearmann's Rho correlation coefficients. The number of nodes used in the statistical calculation is shown in the table, and all values are significant to < 0.05 level.

		Number of nodes	Zonal and Transient source Spearmann's Rho	Point and Transient source Spearmann's Rho
Ventilation regime A				
z–z Source	$Y = 1.15$ m	13,405	0.97	0.75
	$Y = 1.60$ m	10,688	0.98	0.81
x–x Source	$Y = 1.15$ m	13,800	0.96	0.54
	$Y = 1.60$ m	10,690	0.94	0.67
Ventilation regime B				
z–z Source	$Y = 1.15$ m	11,180	0.97	0.67
	$Y = 1.60$ m	9111	0.97	0.65
x–x Source	$Y = 1.15$ m	11,800	0.99	0.55
	$Y = 1.60$ m	9111	0.99	0.45

Table 4
Particle deposition as a percentage of injected for each source definition for the numerical validation.

	Zonal	Transient	Point
Regime A			
Source x–x	54	54	56
Source z–z	70	69	71
Regime B			
Source x–x	67	94	55
Source z–z	59	68	56

3.3. Application and sensitivity of the zonal source

In order to assess the sensitivity of the zonal source geometry and the point source location the scalar concentration at three points around the bed (Fig. 3) was determined for each of the 15 sources. Fig. 13 shows the concentrations at the three sample points and the variation between the point sources, and the zonal sources separately. It is clear that the risk at position S2 varied greatly depending on the source position, moving the source only 0.5 m gives a very different concentration pattern as can be seen in Fig. 14 with concentration changing from 96 to 24 cfu m^{-3}.

For the particle tracking model Fig. 15 shows the wide variation in the quantity of particles extracted from the space using a point source in comparison to the zonal source. The influence of source location appears to increase with particle size, with the 20 mm particles results showing a difference of nearly 80% depending on the location of the point source. However, the variation caused by changing the size of the zonal source is also over 20% for these larger particles which although less is still significant.

4. Discussion

It is common practice to represent the source of bioaerosols in hospital ward models by a central point source at the head of the bed, however it should be recognised that significant hospital pathogens such as MRSA can colonise the skin and become dispersed into the air during regular nursing activities. These releases of bacteria occur across large spatial areas and are subject to a significant amount of variation. A single transient simulation of such a release would only represent one possible scenario, whereas in reality there are infinite variations in the transient release due to the nature of the human behaviour. Therefore it is useful to be able to represent the average dispersion pattern of such releases and the above study has demonstrated how this type of dispersal may be approximated in a steady state CFD model The results presented suggest that a zonal source is likely to yield more realistic results than a point source for such releases, however it should be acknowledged that the findings are not based on an exhaustive study and the zonal source should be used with care. Some of the key limitations of the study are outlined further in the discussion below.

4.1. Experimental validation of the CFD methodology

The experimental validations shown here are important as they present controlled experimental conditions designed to directly mimic the CFD model incorporating bioaerosol transport, as opposed to validating simulated bioaerosol transport to tracer gases which is more common. They also consider the pattern of dispersal across the space, indicating areas of higher or lower risk,

rather than a total or representative biological count in the room. Since the experiments were carried out using microorganisms there was a large amount of variation in sampled counts between locations. However despite this the simulations gave a reasonable representation of the results. The contour plots (Fig. 7) show clearly the similarities between the model and the experimental results and in particular the tendency for the bioaerosols to be entrained towards the inlet air stream in both cases. The CFD simulation shows a 'safe' zone down the side of the room, with a much lower level of contamination than is shown in the experimental results. This is mainly due to the lower resolution in the experimental data where concentrations were not measured close to the wall.

Although the k-ε turbulence model is well validated for use to simulate bulk air flow, this is not the case for particle tracking simulation, and particularly deposition. In fact the assumption of isotropic turbulence has been found to overestimate the deposition of small particles <1 μm in diameter [32], with results becoming more realistic as inertial forces dominate with large particles. There is a lack of literature presenting experimental data on the deposition of bioaerosols however there have been some attempts to validate the deposition of particles. Leduc and Fredriksson [43] replicated the deposition within a particle sampler and found the RNG turbulence model gave improved results for the deposition of particles <1 μm. However in this study of a full scale room no significant difference was found for the deposition with the two different turbulence models for particles this size. Rui et al. [35] attempted to correlate the simulated deposition of bioaerosols to the transport of bacteria that occurred during a knee surgery. However the level of movement present in the real situation is attributed to lack of correlation between the two scenarios.

In the study presented here bioaerosol deposition was measured in a room-size test chamber, under controlled conditions, to ensure

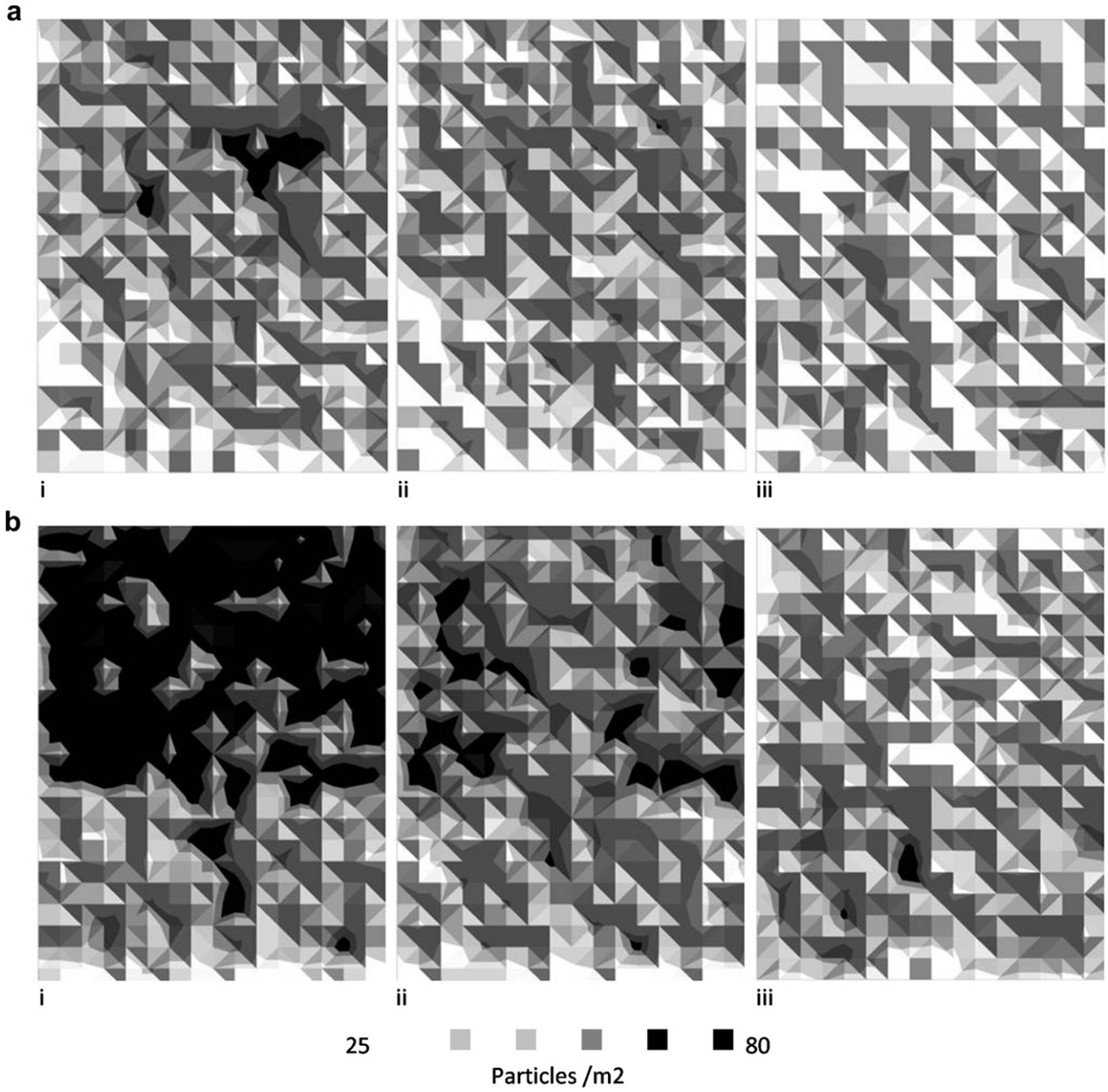

Fig. 12. Deposition patterns from CFD simulation across the chamber floor for (a) 5 μm and (b) 10 μm particles for (i) Transient, (ii) Zonal and (iii) Point source respectively. Results shown for ventilation regime B and the z–z source. Orientation as plan in Fig. 1.

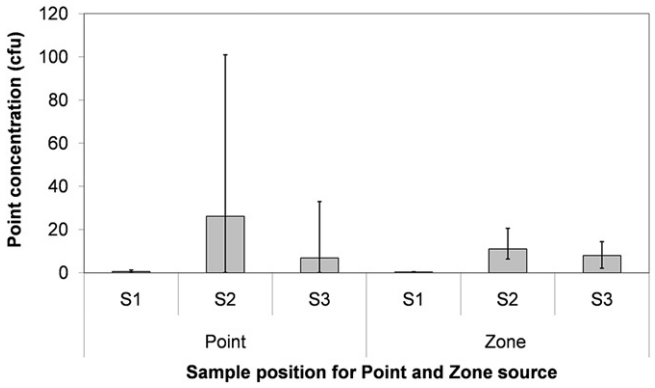

Fig. 13. Average and range (error bars) of concentrations found at each sample point in model 3 for all point and zonal source definitions.

the simulations were directly comparable to the experiments. The study considered the overall deposition of a range of particles with a mass median diameter of 2.5 μm and found the results to be comparable between the simulation and experiments, but only when the DRW model was incorporated into the particle tracking model. Since the aim of the zonal source is to simulate average behaviour of a bioaerosol source it may be expected that using simply the effect of the bulk airflow on the particle would provide adequate results. However, without incorporating the DRW model the deposition was significantly underestimated. These results are promising, indicating that simple passive scalar and particle tracking approaches within steady state CFD models may be used to understand the behaviour of bioaerosols. However to understand the effect of turbulence on smaller particles further work is required. The validation also does not consider the pattern of deposition across the space which is important to understand where pathogenic particles may land and cause reservoirs of infection within a ward. However this study provides an important step in validating CFD models to the airborne dispersion and the total deposition of bioaerosols within a room.

4.2. Numerical validation of the zonal source

Although the increase in computing power has meant the impact of occupant movement on airflow is beginning to be incorporated within CFD models, it would be impossible to model all the variations in nurse, or patient movement and the resulting bacteria release. The zonal source is an attempt to respond to this situation by providing a way of representing an important source of bacteria in a hospital in a manner which represents the inherent assumptions required when simulating such a scenario. It is clear from the numerical simulation described above that the average behaviour of the steady state zonal source correlates very well to the average behaviour of a transient source. Therefore this simple representation of the dispersal could provide valuable results to improve understanding of bioaerosol transport within hospitals. As well as taking significantly less time and effort to generate the simulation, the simple results from a steady state simulation convey the average behaviour of the scenario rather than presenting misleadingly complex results from a transient model of an uncertain situation. Although the point source showed a reasonable representation of the moving source in one of the air flow regimes the results exhibited more case dependence than the zonal source. Since it is not possible to know whether it would be representative without carrying out transient simulations for comparison it should be assumed that the point source will not be suitable for simulating the release of bacteria during activity that has a significant spatial component, as in certain air flow regimes it can give highly erroneous results. However, despite the clear improvement in correlation to the time averaged dispersal with the zonal source this validation only represents an initial test with a continuous release from a single point source traversing the space with a constant speed. The zonal source has not been compared to a point source with different velocities, directional changes, or one whose injection concentration varies in time. Equally, although the point source shows much greater case dependency this is based on only two airflow regimes. With other ventilation configurations such as local extract or displacement ventilation the results may differ.

4.3. Application and sensitivity of bioaerosol sources

CFD may be used within a space to optimise design or compare the risk to patients and staff with different ventilation regimes and room layout [14,20,44]. However with certain regimes, particularly when there is less mixing, the location of the source can have a significant effect on the evaluated risk reduction. This is important because patients themselves move, as do hospital beds. It is therefore quite feasible that the location of the bioaerosol source will move. Small movements of source location, particularly with strong directional airflows can have large effects on the risk to HCWs as shown in the sensitivity study. As such it is imperative to carry out sensitivity studies to understand how the risk evaluation changes with source location.

The geometry of the zone in which bacteria is released during activity will vary each time the activity is performed. For instance every time a bed is made the movements will vary to some extent. Therefore an exact zone can never be defined, and it is important to understand the implications that the assumption of zone size and shape will make. Considering Figs. 13 and 15, the zonal source gives reasonably similar results for changes in volume over the top of the bed. However when the source is very thin there are very high

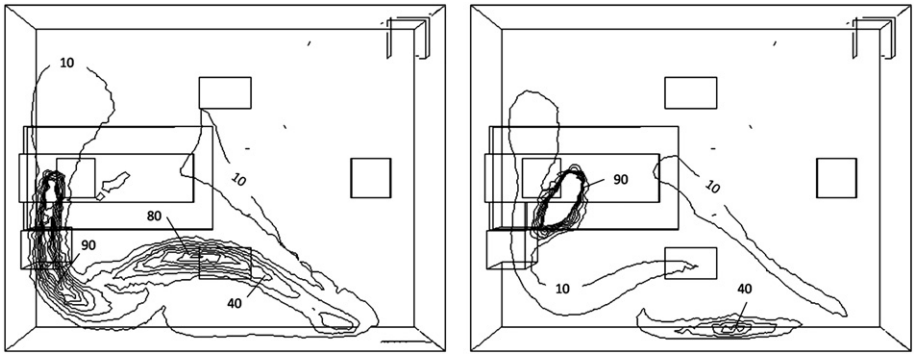

Fig. 14. Contours of bioaerosols from two point sources released at point B (left) and E (right). Values shown are in cfu/m^3.

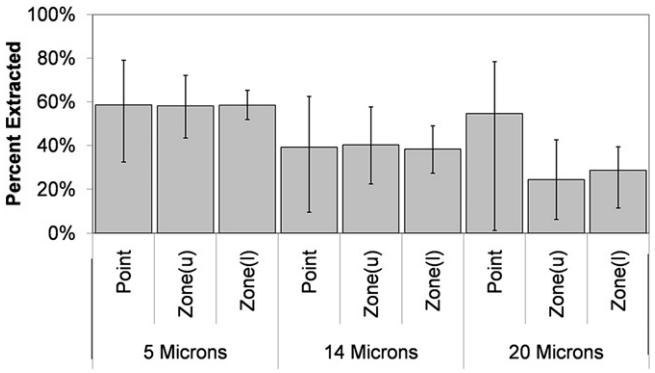

Fig. 15. Average and range of particles extracted in three size ranges from the room using different point source locations, or zonal source dimensions.

concentration values near the bed and with the particle tracking model there is much greater deposition onto the bed. Since the turbulence model is known to overestimate the velocities perpendicular to the wall [32] it is not surprising that when all the particles are injected 2 or less cells away the rates of deposition are high. Care should therefore be taken to ensure the zonal source is thicker than the width of two cells.

The zonal source in the sensitivity study only considered activities occurring over the bed such as bedmaking which has long been recognised as dispersing large amounts of bacteria into the air [10]. Through observations on a four bed hospital bay the authors found that the highest levels of airborne bioaerosols corresponded to dealing physically with the patients which occurred behind curtains and either on, or next to the bed [45]. By using the zonal source in such situations it is possible to improve understanding of the risk of infectious particles travelling to other patients' areas and being deposited on other beds or side tables where they may be responsible for indirect contact transmission. This study has only assessed the sensitivity of such a source for bedmaking, and hence use for other activities should be carried out with due consideration for the realism of the geometry and the sensitivity of the solution to variation in geometry.

This paper has discussed the dispersion of bacteria during nursing activities, however these activities also affect the air flow in the space promoting mixing and the movement of infectious material between areas particularly in situations with low mixing [46] such as local exhaust or displacement ventilation where the directionality, or thermal stratification is the design intent [47,48]. There are attempts to incorporate human movement into airflow models e.g [37]. However despite being more accurate and detailed for the single motion that is being simulated these will not provide a good understanding of how an isolation room performs in practice when the nurse will move in many different ways. Brohus et al. [49] recognised this and attempted to replicate both the average and worse case scenario of HCWs movement within a steady state model of an operating theatre. He created zones with sources of momentum for the person moving through the space. Following this initial validation of time averaging to represent the dispersal of bacteria due to movement it would be beneficial to link this with the ideas laid out in Brohus et al. [49] to incorporate both the effects on bacterial dispersal and the resulting changes to the air flow from the nursing activities within a ward.

5. Conclusion

Both passive scalar transport and particle tracking models within a steady state CFD simulation have been shown to compare well to the overall pattern of airborne spatial distribution and total deposition of bioaerosols in a ventilated space. The experimental comparison is limited to the behaviour of small diameter ($\sim$2.5 mm) bioaerosols and loss of viability generates large variability in the experimental data. However, the results give increased confidence that both approaches are appropriate for representing the dispersion of airborne pathogens in indoor environments.

The zonal source has been shown to provide a good representation of the time averaged dispersion of a transient source using passive scalar transport and to be representative of total deposition and extraction of particles when using a particle tracking approach with a DRW model for the cases presented here. A point source was not a good representation of a transient source, except in specific flow patterns.

It is recommended that when using CFD to understand the effect of hospital ward design and ventilation methods the pathogen source should be carefully considered. If the space is not only for respiratory patients, it is necessary to consider the dispersal of bacteria from other sources including nursing activities. For this situation a zonal source encompassing the area of activity may give a better representation of the average risk. Even in situations where the space is being specifically designed for respiratory diseases, such as TB, it is necessary to consider the sensitivity of the source location especially when using directional ventilation systems.

Acknowledgements

This study was carried out as part of a PhD studentship funded by the EPSRC through a departmental training account.

References

[1] Centers for Disease Control and Prevention. Guidelines for preventing the transmission of *Mycobacterium tuberculosis* in Health-Care settings, 2005. MMWR 2005;54 (No. RR-17, 1-141).
[2] Williams REO. Epidemiology of airborne Staphylococcal infection. Bacteriol Rev 1966;30(3):660–74.
[3] White A. Relation between quantitative nasal cultures and dissemination of Staphylococci. J Lab Clin Med 1961;58(2):273–7.
[4] Dietzer B, Rath A, Wendt C, Martiny H. Survival of MRSA on sterile goods packaging. J Hosp Infect 2001;49(4):225–61.
[5] Neely N, Maley MP. Survival of Enterococci and Staphylococci on hospital Fabrics and Plastics. J Clin Microbiol 2000;38(4):724–6.
[6] Boswell TC, Fox PC. Reduction in MRSA environmental contamination with a portable HEPA-filtration unit. J Hosp Infect 2006;63(1):47–54.
[7] Duguid JP, Wallace AT. Air infection with dust liberated from clothing. Lancet 1948;252(6535):845–9.
[8] Mackintosh CA, Lidwell OM, Towers AG, Marples RR. The dimensions of skin fragments dispersed into the air during activity. J Hyg-Cambridge 1978;81: 471–9.
[9] Davies RR, Noble WC. Dispersal of bacteria on desquaminated skin. Lancet 1962;2(7269):1295–7.
[10] Walter CW, Kundsin RB, Sholkret MA, Day MM. The spread of Staphylococci to the environment. Antibiot Annu 1958;6:952–7.
[11] Shiomori T, Miyamoto H, Makishima K, Yoshida M, Fujiyoshi T, Udaka T, et al. Evaluation of bedmaking-related airborne and surface methicillin- resistant *Staphylcoccus aureus* contamination. J Hosp Infect 2002;50(1):30–5.
[12] Noble WC, Davies RR. Studies on dispersal of Staphylcocci. J ClinPathol 1965; 18(1):16–9.
[13] Hambraeus A. Transfer of *Staphylococcus aureus* via nurses uniforms. J Hyg–Cambridge 1973;71(4):799–814.
[14] Noakes CJ, Sleigh PA, Escombe AR, Beggs CB. Use of CFD analysis in modifying a TB ward in Lima, Peru. Indoor Built Environ 2006;15(1):41–7.
[15] Li Y, Huang X, Yu ITS, Wong TW, Qian H. Role of air distribution in SARS transmission during the largest nosocomial outbreak in Hong Kong. Indoor Air 2005;15(2):83–95.
[16] Beggs CB, Kerr KG, Noakes CJ, Hathway EA, Sleigh PA. The ventilation of multiple-bed hospital wards: review and analysis. Am J Infect Control 2008; 36(4):250–9.
[17] Chao CYH, Wan MP. A study of the dispersion of expiratory aerosols in unidirectional downward and ceiling-return type airflows using a multiphase approach. Indoor Air 2006;16:296–312.
[18] Chow TT, Yang XY. Performance of ventilation system in non-standard operating room. Build Environ 2003;38(12):1401–11.

[19] Richmond Bryant J. Transport of exhaled particulate matter in airborne infection isolation rooms. Build Environ 2009;44(1):44–55.
[20] Kao PH, Yang RJ. Virus diffusion in isolation rooms. J Hosp Infect 2006;62(3):338–45.
[21] Yu ITS, Li YG, Wong TW, Tam W, Chan AT, Lee JHW, et al. Evidence of airborne transmission of the severe acute respiratory syndrome virus. New Engl J Med 2004;350(17):1731–9.
[22] Noakes CJ, Sleigh PA, Fletcher LA, Beggs CB. Use of CFD modelling to optimise the design of upper-room UVGI disinfection systems for ventilated rooms. Indoor Built Environ 2006;15(4):347–56.
[23] Chung K, Hsu S. Effect of ventilation pattern on room air and contaminant distribution. Building Environ 2001;36(9):989–98.
[24] Huang JM, Chen QY, Robit B, Rivoalen H. Modelling contaminant exposure in a single-family house. Indoor Built Environ 2004;13(1):5–19.
[25] Khan JA, Feigley CE, Lee E, Ahmed MR, Tamanna S. Effects of inlet and exhaust locations and emitted gas density on indoor air contaminant concentrations. Build Environ 2006;41(7):851–63.
[26] Zhang Z, Chen X, Sagnik M, Zhang T, Chen O. Experimental and numerical investigation of airflow and contaminant transport in an airliner cabin mock-up. Helsinki, Finland. In: Proceedings of Roomvent; June 13–15 2007.
[27] Chang TJ, Hsieh YF, Kao HM. Numerical study of the effect of ventilation pattern on coarse, fine and very fine particulate matter removal in partitioned indoor environment. JAPCA J Air Waste Ma 2007;57:179–89.
[28] Lu W, Howarth AT. Numerical analysis of indoor aerosol particle deposition and distribution in two-zone ventilation system. Build Environ 1996;31(1):41–50.
[29] Zhang Z, Chen Q. Experimental measurements and numerical simulations of particle transport and distribution in ventilation rooms. Atmos Environ 2006;40:3396–408.
[30] Zhao B, Yang C, Yang X, Liu S. Particle dispersion and deposition in ventilated rooms: testing and evaluation of different Eulerian and Lagrangian models. Build Environ 2008;43:388–97.
[31] Wan MP, Chao CYH, Ng YD, Sze To GN, Yu WC. Dispersion of expiratory droplets in a general hospital ward with ceiling mixing type mechanical ventilation system. Aerosol Sci Tech 2007;41(3):244–58.
[32] Lai ACK, Chen FZ. Modelling particle deposition and distribution in a chamber with a two-equation Reynolds-averaged Navier-Stokes model. J Aerosol Sci 2006;37(12):1770–80.
[33] Noakes CJ, Fletcher LA, Sleigh P, Booth W, Beato-Arribas B, Tomlinson N. Comparison of tracer techniques for evaluating the behaviour of bioaerosols in hospital isolation rooms. In: Healthy Buildings; 2009. Syracuse, New York, USA. September 13 to 17, 2009.
[34] Grinshpun SA, Adhikari A, Honda T, Kim KI, Toivola M, Rao R, et al. Control of aerosol contaminants in indoor air: combining the particle concentration reduction with microbial inactivation. Environ Sci Technol 2007;41(2):606–12.
[35] Rui Z, Guangbei T, Jihong L. Study on biological contamination control strategies under different ventilation models in a hospital operating room. Build Environ 2008;43(5):793–803.
[36] Liu J, Wang H, Wen W. Numerical simulation on a horizontal airflow for airborne particles control in hospital operating room. Build Environ 2009;44(11):2284–9.
[37] Shih YC, Chiu CC, Wang O. Dynamic airflow simulation within an isolation room. Build Environ 2007;42(9):3194–209.
[38] Rosebury T. Experimental airborne infection. Baltimore: Williams and Wilkins Company; 1947. 3033.
[39] Macher JM. Positive-hole correction of multiple-jet impactors for collecting viable microorganisms. Am Ind Hyg Assoc J 1989;50(11):561–8.
[40] NHS Estates. HBN4 Supplement 1: isolation facilities in acute settings. London: The Stationary Office; 2005.
[41] Noble WC, Lidwell OM, Kingston D. The size distribution of airborne particles carrying micro-organisms. J Hyg-Cambridge 1963;61(4):385–91.
[42] BGI Collinson Nebulizer. Output distribution of the collison nebulizer, http://www.bgiusa.com/agc/output_distribution.htm; 2006 [accessed March 2011].
[43] Leduc S, Fredriksson C, Hermansson R. Particle tracking option in Fluent validated by simulation of a low pressure impactor. Adv Powder Technol 2006;17(1):99–111.
[44] Chau OKY, Liu CH, Leung MKH. CFD analysis of the performance of a local exhaust ventilation system in a hospital ward. Indoor Built Environ 2006;15(3):257–71.
[45] Hathway EA, Fletcher LA, Noakes CJ, Sleigh PA. Bioaerosol production from routine activities within a hospital ward. Proceedings of the 11th International Conference on Indoor Air Quality and Climate: Indoor Air 2008. August 17-22; Copenhagen, Denmark.
[46] Tang JW, Eames I, Chan P, Ridgeway GL. Factors involved in the aerosol transmission of infection and control of ventilation in healthcare premises. J Hosp Infect 2006;64(2):100–14.
[47] Matsumoto H, Ohba Y. The influence of moving object on air distribution in displacement ventilated rooms. J Asian Archit Build Eng 2004;3(1):71–5.
[48] Bjorn E, Nielsen PV. Dispersal of exhaled air and personal exposure in displacement ventilated rooms. Indoor Air 2002;12(3):147–64.
[49] Brohus H, Balling KD, Jeppesen D. Influence of movements on contaminant transport in operating room. Indoor Air 2006;16(5):356–72.